Linear and Nonlinear Springing Analyses in Time Domain using a Fully Coupled BEM-FEM

Yooil Kim, Kyong-Hwan Kim, Yonghwan Kim
Seoul National University, Seoul, Korea

1. Introduction

Global hydroelasticity of modern merchant ship is gathering a lot of attention due to the rising concerns about its negative impact on design of sound structure especially in terms of unexpected increase of design load as well as fatigue loading. Recent experiences from a real ship in operation tell that cracks are observed at bracket toe in deck longitudinal in way of transverse bulkhead after one year of operation in the North Atlantic (Storhaug, 2007). The ship was made of class-certified high tensile steels, HTS36, meeting IACS's rule requirements. Based on the measurement through onboard hull monitoring system, it was concluded that these cracks were caused by continuous wave induced vibration. In addition to the fatigue damage, this resonant vibration as well as transient vibration due to bow slamming also has significant impact on the increase of extreme wave bending moment threatening the safety level of seagoing vessels. However, current rule requirements do not take into account this type of vibration induced fatigue damage and extreme wave load in ship design leaving potential catastrophic failures ahead of us.

In this study, a new approach which combines both BEM and FEM directly in time domain is taken. What distinguishes the current time domain approach from previously studies is that current approach handles BEM and FEM in time domain directly without relying on the inverse Fourier transform of frequency domain solution introduced by many others so far. Moreover, the solution of finite element equation is sought by using direct integration method, not by modal decomposition method mentioned above. The most popularly used direct integration scheme, Newmark-β method, which is a unconditionally stable implicit method of the second-order accuracy is used to discretize finite element equation in time.

2. Theoretical Background

For the solution of fluid part, a time-domain Rankine panel method is used. In this method, solution variables such as potential and its normal derivatives etc., are discretized in space by using bi-quadratic B-spline function, so that continuity up to its second derivatives are guaranteed across each panel. Linearized body boundary condition derived by Ogilvie and Tuck(1969) is applied to flexible body by using modified Nakos approach. In doing so, the approach introduced by Nakos, where Stokes theorem is used for the calculation of second derivative of basis potential in m-terms, is modified to take into account the arbitrary deformation pattern of the flexible body. Eqn(1) shows Stokes theorem applied to source term of the integral equation. M-term in Eqn(1) contains second derivative of basis potential and is converted into first derivative as shown.

$$\iint_{S_B} m_j(Q)G(P,Q)dS_B = -\iint_{S_B} \left(\nabla\Phi(Q)\cdot\nabla G(P,Q)\right)n_j dS_B \tag{1}$$

This original Nakos approach was slightly modified in order to apply it to flexible body case. Firstly, whole ship is artificially divided into several segments along it length. Then, an assumption that strain tensor inside each segment is neglibly small so that each segment can be treated like rigid one was introduced in this stage. This assumption is reasonable because, first of all, the length of segment is normally chosen to be very small. Moreover, it is believed to be true that deformation gradient inside each segment would be very small thanks to the relatively high stiffness of general ship structure. Eqn(2) shows the process through which source term of the integral equation is transformed into the one ready to use Stokes theorem.

$$\iint_{S_B} \frac{\partial \phi_d}{\partial n}(Q)G(P,Q)dS_B = \iint_{S_B}\left[\sum_{i=1}^{6}\left(\frac{\partial \xi_i}{\partial t}n_i + \xi_i m_i\right) - \frac{\partial \phi_I}{\partial n}\right]G(P,Q)dS_B$$
$$= \sum_{n=1}^{N}\iint_{S_{Bn}}\left[\sum_{i=1}^{6}\xi_i' \, m_i'(Q)\right]G(P,Q)dS_{Bn} + \iint_{S_B}\left[\frac{\partial \mathbf{u}}{\partial t}\cdot\mathbf{n} - \frac{\partial \phi_I}{\partial n}\right]G(P,Q)dS_B \tag{2}$$

Finally, after applying Stokes theorem mentioned above, m-term which is present in the source term can be expressed in terms of first derivative of basis potential as the summation over the whole segment.

$$\sum_{n=1}^{N}\iint_{S_{Bn}}\xi_1' \, m_1'(Q)G(P,Q)dS_{Bn} = \sum_{n=1}^{N}\xi_1'\left[-\iint_{S_{Bn}}\nabla\Phi(Q)\cdot\nabla_Q G(P,Q)n_1 dS_{Bn} + \oint_{\partial S_{Bn}}\mathbf{dl}\times G(Q)\nabla\Phi(Q)\right]$$
$$= \sum_{n=1}^{N}\xi_1'\left[-\iint_{S_{Bn}}\nabla\Phi(Q)\cdot\nabla_Q G(P,Q)n_1 dS_{Bn}\right] \tag{3}$$

Less tight approach below weak scatterer is weakly nonlinear approach, which is tried in this study. In this approach hydrodynamic pressure, both diffraction and radiation related, is evaluated based on linear theory, but both Froude-Krylov and restoring pressure is evaluated at body exact position. Calculation of these two force components is rather straightforward once body motion is given. For this, additional nonlinear mesh on which nonlinear Froude-Krylov and restoring pressure is to be calculated, is required. Deformation and motion of the floating body is assumed to be small within weakly nonlinear approach. Froude-Krylov(FK) pressure on dry surface under mean water line level is forced to be zero, while the one on wet surface above mean water line is obtained by using Taylor expansion from mean water line.
Eqn(4) shows nodal forces acting in vertical upward direction induced by this body-exact FK pressure. FK pressure without prime indicates the value on mean-body surface, and with prime is the values on exact body surface. Since basis potential is defined on the mean-body surface, coupled terms between basis potential and wave potential have to stay on the mean body even in case of nonlinear formulation.

$$R_{z,i} = \iint_{\bar{S}_{Bi}} p_{FK}n_z N_1 dS - \iint_{\bar{S}_{Bi}} p_{FK}zn_x N_{1,x}dS + \iint_{S_{Bi}} p_{FK}' n_z' N_1 dS - \iint_{S_{Bi}} p_{FK}' z' n_x' N_{1,x}dS$$
$$R_{z,j} = \iint_{\bar{S}_{Bi}} p_{FK}n_z N_3 dS - \iint_{\bar{S}_{Bi}} p_{FK}zn_x N_{3,x}dS + \iint_{S_{Bi}} p_{FK}' n_z' N_3 dS - \iint_{S_{Bi}} p_{FK}' z' n_x' N_{3,x}dS \tag{4}$$

Body-exact restoring pressure can be evaluated by subtracting hydrostatic pressure on initial mean body position from that at current exact body position. Calculation of nodal forces acting on beam nodes can be done in similar way of Eqn(4).
For the solution of structural part, Vlasov beam theory is followed which is able to take into account the effect of warping distortion. The effect of warping becomes very important when the cross section of the ship is thin-walled-open one, which is the case of modern large sized container carriers. Also, the effect of coupling between horizontal bending and torsion which is caused by the gap between neutral axis and shear center locations, is taken into account. These two typical behaviors of thin-walled-open-sectioned beam are critical in that the lowest natural frequency of these container carriers is torsional one and the second lowest one is coupled horizontal bending and torsion. This, in turns, means that those two vibration modes are most likely excited by incoming waves whose frequency level sits right on the spot where the energy of ocean wave is highly packed.
To obtain the solution from above mentioned two coupled equations, an iterative method is used where the solutions of two field equations are exchanged between them until converged solution is obtained. Fixed-point iteration with relaxation method is used to accelerate convergence rate, and the modified Aitken's δ^2 process is used for the determination of optimum relaxation parameter. In seeking the solution of structural FE equation, both modal superposition method and direct integration method are used. In modal superposition method, system equations are treated in modal space whose basis vectors are structure's mode shapes. Therefore, all physical quantities of both fluid and structure domain are projected to this new space through the inner product of related vector and mode shape. In direct integration approach, spatially-discretized structural FE equation is directly discretized in time domain by

using Newmark-β method which is second order unconditionally stable time marching scheme popularly used in structure community.

3. Analysis Results

Some validation works have been done on flexible barge model. Computational results were compared with experimental data which have been obtained by Remy *et al*., and raw data was provided by them through private communication. Free-decay test as well as the response under wave excitation on stationary flexible barge was carried out. Details of this can be found in Kim *et.al.*(2008).

To check the applicability of developed computer program, a more realistic case is handled in this study. Artificial flexible S175 model with open cross section was created with realistic sectional properties to see the response under oblique wave with forward speed. The second moment of inertia in both vertical and horizontal directions was set to be 63.2 and 178 m^4, respectively. Warping constant was set to be 5660 m^6, and St.Venant's torsional constant to be 1.36 m^4. The distance from neutral axis to shear center, which is located far below hull bottom, was 14.7 m. Young's modulus was set to be 200 GPa and Poisson ratio 0.3.

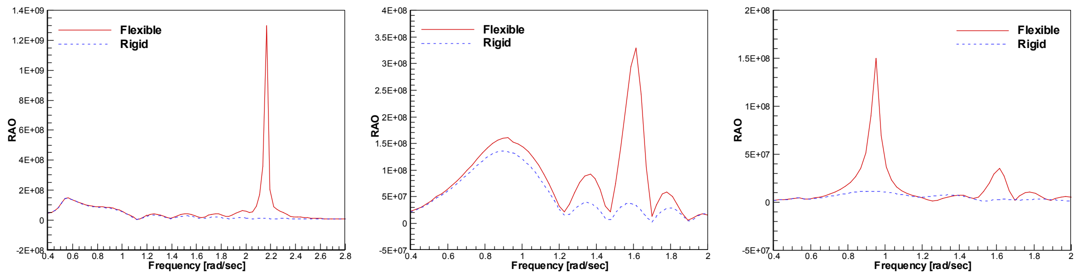

(a) VBM RAO at L/2 (b) HBM RAO at L/2 (c) TM RAO at L/4

Fig.1 Sectional load RAO (Fn=0.275, β=120°)

Fig.1 shows sectional load RAO when wave heading angle is 120°. Vertical 2-node resonance vibration takes place around 2.2 rad/sec. For horizontal bending moment shown in Fig.1(b), resonance vibration occurs at 1.6 rad/sec, where torsional moment at L/4 peaks as well. This means that coupled horizontal bending and torsion is taking place at this frequency level. Torsional moment at midship has its peak at 0.95 rad/sec, which corresponds to twisting vibration mode. Fig.2(a) shows hull deformation when the body goes through twisting mode resonant vibration under 120° heading angle. Solid line without fill is deformed configuration, so that vibration mode can be seen clearly when compared with its original configuration which is filled one. It can be seen that bow and stern rotates in opposite direction while the midship part remains un-rotated. Rather straight keel line vividly shows that horizontal bending is almost absent in this mode. This explains well the presence of sharp peak at this frequency level in Fig.1(c). Little difference of horizontal bending moment between rigid and flexible body in Fig.1(b) demonstrates that vibration induced horizontal bending is almost negligible.

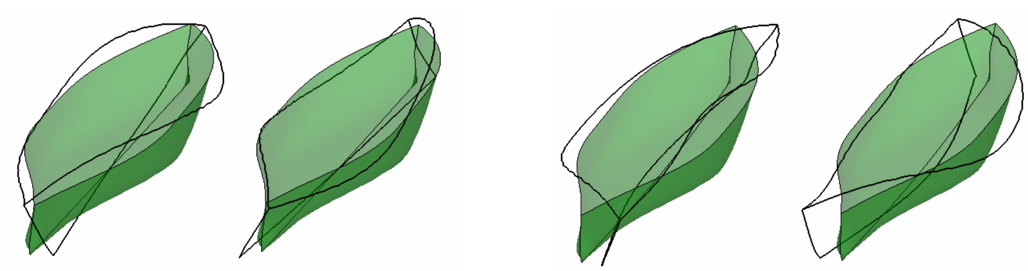

(a) ω=0.95, Fn=0.275, β=120° (b) ω=1.6, Fn=0.275, β=120°

Fig.2 Hull deformation (submerged part only)

Fig.2(b) is the case when wave frequency goes up to 1.6 rad/sec, where coupled horizontal bending and torsion is taking place. Careful attention to the deformed configuration in Fig.2(b) tells that the body is exposed to horizontal bending together with torsion. In this case, bow and stern rotates in same direction whereas midship in opposite direction indicating maximum torsion will be at quarter point, that is to say, both at 3L/4 and L/4. Curved keel line proves that horizontal bending is significant in this mode. It should be noted that deformed shape in Fig. is highly exaggerated because, in reality, deformation magnitude is not visibly big.

Fig.3 shows the comparison of nonlinear vertical bending moment between rigid and flexible bodies when wave frequencies are 0.5 and 1.67 rad/sec respectively. The former one corresponds to the heave resonance frequency of the rigid body, and the latter one to two node vertical bending resonance frequency. It can be seen that flexible resonance frequency component is present when wave frequency is 0.5 rad/sec together with first and second harmonic components. This is because of nonlinearity that restoring force holds implicitly containing all higher order frequency component. When wave frequency is 1.67 rad/sec, vertical bending moment of rigid body becomes very small, as is understandable because wave length is too small in this frequency level. However, when body becomes flexible under same wave frequency, vertical bending moment turned out to be quite large thanks to the resonance between excitation and flexible hull girder response.

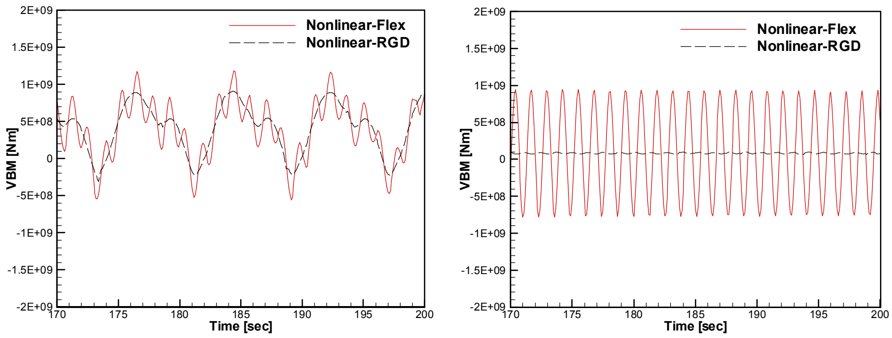

(a) VBM at L/2 (ω=0.5) (b) VBM at L/2 (ω=1.67)

Fig.3 Nonlinear VBM comparison between rigid and flexible body (Fn=0.275, β=180^o, A=3m)

4. Conclusions

Steady-unsteady coupling term of flexible body is successfully incorporated in forward speed case by using modified Nakos approach, so that application was extended to S175 with scaled down structural properties. As a results of it, typical behavior of container carrier came out, that is to say, twisting and coupled horizontal bending and torsion turned out to be the lowest two vibration modes. Weakly nonlinear approach where body exact restoring pressure and Froude-Krylov pressure are taken into account, was tried ending up with highly oscillatory response in wave frequency regime.

Acknowledgement

The present research was supported by Lloyd's Register Educational Trust. Authors appreciate for their support.

References

1. Bishop, R.E.D., and Price, W.G., 1979, *Hydroelasticity of Ships*, Cambridge University Press.
2. Kim, Y., Kim, Y., 2008, "Analysis of springing effects on floating barges in time domain by a fully coupled hybrid BEM-FEM", 23rd IWWWFB, Jeju, Korea
3. Kim, Y., 2008, Time domain analysis on hull-girder hydroelasticity by fully coupled BEM-FEM approach, PhD thesis, Seoul National University, Korea
4. Malenica, S, Molin, B, Remy, F., Senjanovic, I, 2003, "Hydroelastic response of a barge to impulsive and non-impulsive wave loads", Hydroelasticity 2003, Oxford, UK.